Analyst

Accepted Manuscript

ROYAL SOCIETY OF CHEMISTRY

www.rsc.org/analyst

Cite this: DOI: 10.1039/c0xx00000x

www.rsc.org/xxxxxx

PAPER

A dark field light scattering platform for real-time monitoring the erosion of microparticles by Co^{2+}

Hui Yang,[a] Yue Liu,[a] Peng Fei Gao,[b] Jian Wang*[b] and Cheng Zhi Huang*[a,b]

Received (in XXX, XXX) Xth XXXXXXXXX 20XX, Accepted Xth XXXXXXXXX 20XX

DOI: 10.1039/b000000x

Monitoring chemical reactions is crucial for understanding reaction mechanisms in analytical chemistry. In this study, the leaf-like poly (*p*-phenylenediamine) (P*p*PD) microparticles were prepared for highly sensitive sensing of Co^{2+} *via* single microparticle that P*p*PD microparticles as probes. Herein, the dark field microscopy protocol was proved to be a powerful tool for studying the erosive process of microparticles induced by Co^{2+}, which was benefit to deeply understanding the reaction mechanism of analytical chemistry and helpful to expand the applications of dark field microscopy. A possible mechanism was proposed to explain the experimental observations.

Introduction

As one of the essential trace elements for human and many other living creatures, cobalt ion (Co^{2+}) displays double effects on human health.[1] On one hand, Co^{2+} is the ingredient of Vitamin to promote the formation of red blood cells.[2] On the other hand, Cobalt compounds from diet and occupational exposure in several industries such as hard metal industry, diamond polishing, and the porcelain, chemical, and pharmaceutical industries[3] may cause toxicological effects, including diarrhea, flushing, and vomiting in humans and animals.[4,5] Therefore, the development of highly sensitive and selective analytical methodology of Co^{2+} is of great importance, and has attracted increasing attention in recent years. To avoid its toxic effects, high-performance monitoring in industrial, environmental and food sampling is, therefore, required. Currently, several conventional techniques, including spectrophotometry,[6,7] fluorimetry,[8-10] electrochemical sensor,[11-12] chemiluminescence (CL),[13-14] electrochemiluminescence,[15] colorimetric sensors based on functional metal nanoparticls[16,17] and inductively coupled plasma-atomic emission spectrometry (ICP-AES)[18] have been developed to determine Co^{2+}. Some new fluorescent reagents have been synthesized and employed to detect Co^{2+}, [19, 20] but they are restricted by the toxicity of some fluorescent reagents and the complexity of florescence detection systems.

Sensing Co^{2+} with dark-field microscopy (DFM) could be an interesting alternative since the advantages of DFM have been applied for investigating the size, shape, composition and the single particle in local environment.[21-23] In the process of particle preparation, it's inevitable to produce particles of different sizes and shapes that cannot be detected by average measurements. Particles with different size and shape exhibit distinctive chemical and physical properties in spectral bands, reaction activity and efficiency. Measurements from single particle could reflect the unique function of individual particles, which is way better than the average measurements taken from ensemble solutions. DFM is a highly sensitive way to detect analytes effectively and shortly.[24-26] Notably, in addition to high sensitivity, like other single-molecule spectroscopy techniques, every single particle could serve as an independent probe in DFM[27, 28] which provide significant signals with high signal-to-noise ratio[29, 30] and imaging platforms to improve the temporal resolution.

However, the application of DFM for real-time monitoring of corrosion reaction has rarely been studied before.[31-33] Herein, we described a novel method to monitor a Co^{2+}-driven corrosion reaction of single leaf-like poly (*p*-phenylenediamine) (P*p*PD) microparticle by DFM, wherein a shape and scattering color change could be observed, and the corrosion of the P*p*PD persisted for a finite period time, then the leaf-like structure collapsed gradually to form irregular fragments.

Large particles eroded in a liquid is of intrinsic scientific interest as well as being important in practice. The strategy is shown in Scheme 1, it can be utilized to monitor the erosion dynamics of P*p*PD microparticles induced by Co^{2+}, especially at the single particle level. The erosion of P*p*PD was confirmed by multiple characterizations containing SEM, FTIR, and DLS. During the erosion process, the scattering lights of P*p*PD decrease in intensity and the morphology became smaller. The erosion of P*p*PD underwent two stages: first, rapid adsorption of Co^{2+} into P*p*PD microparticles; second, quick diffusion of Co^{2+} into P*p*PD microparticles, leading to the breakdown of P*p*PD microparticles.

Experimental Section

Reagents

PVP, [poly (-*N*-vinylpyrrolidone), Mw=55000] was purchased from Sigma. *p*-Phenylenediamine (*p*-PDA) monomer and cobalt chloride ($CoCl_2 \cdot 6H_2O$) were gotten from Sinopharm Chemical Reagent Co, Ltd. (Shanghai, China). Chloroauric acid tetrahydate ($HAuCl_4 \cdot 4H_2O$) was purchased from Sinopharm Chemical

Reagent Co, Ltd. (Shanghai, China). Other chemicals were analytical reagent grade used without further purification. Milli-Q purified water (18.2 MΩ at 25 °C) was used for all sample preparations.

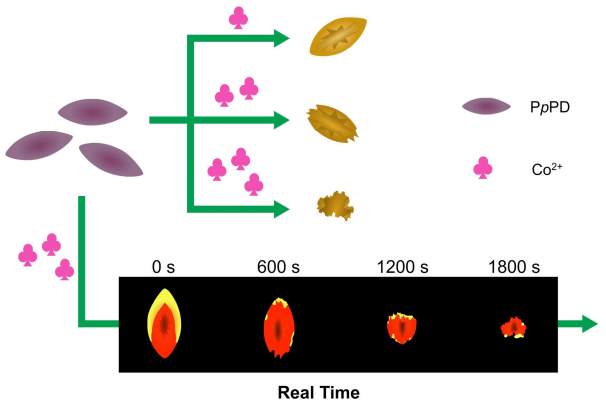

Scheme 1. Schematic illustration of the strategy for Co^{2+} detection using P*p*PD leaf-like microparticals approach.

0.1 g/mL PVP working solution and 0.05 g/mL *p*-PDA working solution were prepared respectively by directly dissolving in doubly distilled water under vigorous magnetic stirring, and homogeneous solution at room temperature was available as a consequence. 1% $HAuCl_4$ working solution was obtained by dissolving 1 gram $HAuCl_4$ powder in a 100 mL volumetric flask.

Apparatus

Dark-field light scattering (DFLS) imaging was carried out through BX51 optical microscope (Olympus, Japan) equipped with a high numerical dark-field condenser (U-DCW, 1.2-1.4). The scattering light was collected by a 100×object lens and images were taken by DP72 single chip truecolor CCD camera (Olympus, Japan) controlled by IPE software. The images were analyzed with Image-Pro Plus (IPP) software (Media Cybernetics, America). The scan electron microscopy (SEM) images were obtained by a Hitach (Tokyo, Japan) S-4800 microscopy to investigate the size and morphology of the P*p*PD microcrystals. Fourier Transform Infrared (FT-IR) spectra were recorded by a Fourier transform infrared Spectrometer (Shimadzu, 8400S, Japan) from 4000 to 500 cm^{-1} at room temperature. A Malvern Zetasizer Nano instrument (United Kingdom) was used to evaluate the size change of P*p*PD microcrystals. A vortex mixer QL-901 (Haimen, China) was employed to blend the solutions.

Preparation of P*p*PD microcrystals

P*p*PD microcrystals were prepared by the reported methods.[34] Briefly, 1 mL 0.1 g/mL PVP solution and 6 mL 0.05 g/mL *p*-PDA solution were mixed with 2 mL Mili-Q purified water. Then 2 mL of 1% $HAuCl_4$ was added to the solution under continuous stirring for about 3 h at room temperature. After that, the products were centrifuged at 12000 rpm for 10 min and washed 3 times with Mili-Q purified water. Finally, the P*p*PD microcrystals were suspended in distilled water as the stocking solution.

Dark-field light scattering imaging of P*p*PD

To observe the scattering features of P*p*PD reacted with different concentrations of Co^{2+}, we employed a homemade device, which is consisted of slide glass and cover glass to produce a simulative flow cell. Dark-field light scattering images of P*p*PD were taken by depositing P*p*PD to the bottom of the cell. An area containing P*p*PD was selected for real-time study. After dark-field scattering imaging of P*p*PD, Co^{2+} solution was added into the cell to initiate the corrosion of P*p*PD. Then, dark-field scattering images of the same area were obtained at different time as indicated in the text. All the images demonstrate the monitoring of a consecutive corrosion of P*p*PD. The other metal ions were tested and compared under the same conditions as above mentioned.

Data analysis

The caculation of scattering intensity of P*p*PD was carried out through Image-Pro Plus (IPP) software.

Results and Discussion

Characteristics of as-prepared P*p*PD microparticles

The as-prepared leaf-like microparticles presented smooth surface as shown in the typical SEM images (Fig. 1a) with the length about 3 μm and width about 1 μm, and coexist a few spherical gold nanoparticles simultaneously. The X-ray photoelectron spectroscopy (XPS) spectral measurements showed that the microparticles were mainly composed of four elements, Au, C, O, and N (Fig.1b). The binding energy of Au in the P*p*PD microparticles at 84.2 eV and 87.6 eV were ascribed to Au $4f_{7/2}$ and Au $4f_{5/2}$ respectively, which matched with the XPS band of metallic Au^0,[35,36] indicating that gold atoms in P*p*PD microparticles only be present in the form of Au^0.

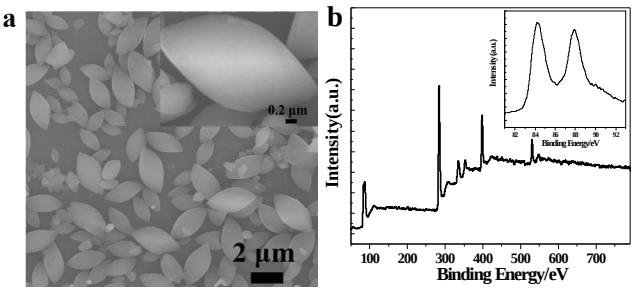

Fig. 1 SEM image (a) and XPS spectra (b) of the as-prepared P*p*PD microcrystals. The insert shows the further magnified SEM image of P*p*PD (a) and the Au $4f_{7/2}$ and Au $f_{5/2}$ doublet, respectively.

Interaction of P*p*PD microparticles with Co^{2+}

Similar with the previous report,[6] P*p*PD microparticles could be eroded through the diffusion of Co^{2+} into P*p*PD microparticles. In this work, the erosion process of P*p*PD microparticles induced by Co^{2+} was monitored by DFM (Fig. 2). Initially, under a white light source, P*p*PD microparticles could scatter strong red light along their edges or sharp corners (Fig. 2a), resulting in the large light scattering cross section of gold.[22] Immediately, after the addition of Co^{2+}, local disintegration was started at the edge of the P*p*PD, which presented a weaker light scattering with smaller size (Fig. 2d). Co^{2+} is the main driving force of corrosion reaction, the light scattering of P*p*PD then decreased steadily as

shown in Fig. 2e, which was due to the adsorption and diffusion of Co^{2+}. Close observation revealed that whenever the erosion reaction occurred, there were apparent residual fragments of P*p*PD existed on the glass slide. It could be interpreted as follows: after the addition of Co^{2+}, not all the surface of P*p*PD is filled up with Co^{2+}, leading to different degrees erosion of P*p*PD.

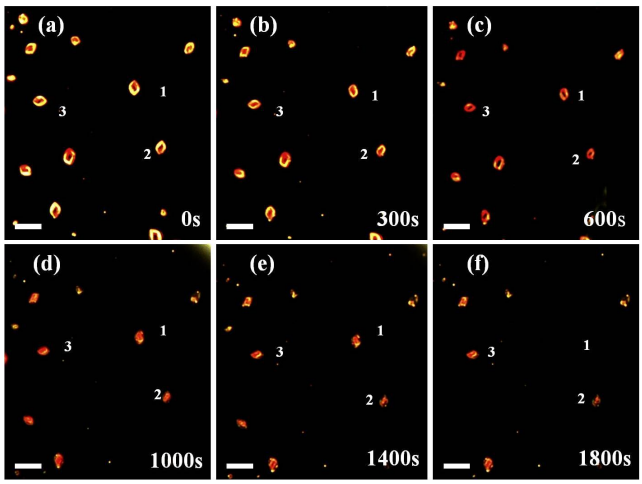

Fig. 2 Dark-filed image of P*p*PD undergoing corrosion by Co^{2+}. The times at which the different images were captured are shown with latency time of 300/400 s. $c_{Co^{2+}}$, 1×10^{-3} mol/L. The scale bar is 3 μm for all images.

To validate the time-dependent shape change of P*p*PD microparticles, SEM images were captured to observe the shape by keeping Co^{2+} at a given concentration but prolonging the reaction time (Fig. S1†), which were consistent with the result obtained from DFM. Moreover, the aqueous solution appeared to be purple and displayed two characteristic UV absorption peaks at 345 and 541 nm, respectively (Fig. 3a). After interacted with Co^{2+}, it resulted in a new absorption peak of P*p*PD at 464 nm, instead of the previous two characteristic absorption peaks. The FTIR (Fig. 3b) measurement clearly proved that the main characteristic peaks of P*p*PD microparticles included the stretching vibrations of the –NH- group at 3461, 3421 and 3333 cm^{-1}, the C=N and C=C stretching vibration in the phenazine ring at 1607 and 543 cm^{-1} respectively. The peaks at 1277 and 1229 cm^{-1} represented the C-N stretches in the benzenoid and quinoid imine units (-C-N-), respectively. These results were in agreement with the frequencies reported earlier.[28] After Co^{2+} added, all the characteristic peaks disappeared, which mean that the initial structure of P*p*PD were broken by Co^{2+}.

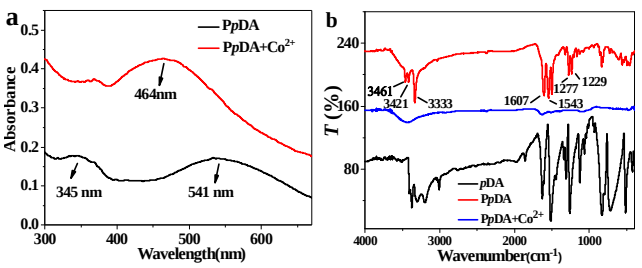

Fig. 3 UV-vis spectra (a) and FTIR spectra (b) of the P*p*PD microcrystals before and after reacted with Co^{2+}. $c_{Co^{2+}}$, 1×10^{-3} mol/L.

To better understand how and why P*p*PD collapsed, it makes sense to consider the formation of P*p*PD, which was extremely similar to the previous report.[28] At very first beginning, *p*DA may induce the formation of oligomeric, and these oligomers, directed by the PVP surfactant developed into the P*p*PD polymer microparticles. Addition to the main interaction between P*p*PD and Co^{2+} as the previous literature reported,[6] it is also related with the electric potential difference of gold ions and cobalt ions.[37,38] Similar with the Ag-Hg system,[32] P*p*PD microparticles and Co^{2+} can be interacted through the diffusion of Co^{2+} into P*p*PD microparticles because the electrode potential for Co is -0.28 V, while Au is 1.002 V. Therefore, the P*p*PD microparticles, initially kept leaf-like structure until they exposure to Co^{2+}, after being incubated for 5 min, the shape and scattering light of P*p*PD changed significantly. The corrosion reaction between P*p*PD and Co^{2+} were irreversible.

We expect that this is a reasonable description of the mechanism in the experimental system. Once the Co^{2+} solution was added, the erosion reaction of P*p*PD happened immediately. Moreover, with a higher concentration of Co^{2+}, more Co^{2+} were adsorbed on the P*p*PD, as a result, the shape of P*p*PD was broken significantly. It may be speculated that Co^{2+} diffused into P*p*PD microparticles and broke off them from the center, widening the sides further, according to the observed SEM images.

Real-time monitoring the corrosion process of P*p*PD microparticles reaction with Co^{2+}

Then we turned to real-time monitoring of the in situ corrosion reaction between P*p*PD and Co^{2+}, which recorded the real-time shape changes and light scattering images of the consecutive corrosion process. The corrosion behavior in movie S1 displayed the typical light scattering images of P*p*PD microparticles after exposure to Co^{2+} solution. After the addition of Co^{2+}, almost all P*p*PD microparticles exhibited shape changes immediately, suggesting the beginning of the corrosion reaction. During the initial stage (within 300 s), noticeable broken structure of single P*p*PD microparticle was observed. After the treatment for 1800 s, almost all P*p*PD microparticles turned out to be irregular with weak light scattering.

To demonstrate the selectivity of Co^{2+} for using the proposed method, a series of other cations were tested under the same conditions. The Fig. S2 showed only Co^{2+} led to a significant scattering change of P*p*PD, however no obviously changes were observed in the experiments employing other cations. The research results indicated the specificity of Co^{2+} for using this method.

Analytical performance

The above results implied the chemical information of prepared microparticles, which might be useful applications in sensing Co^{2+}.[39] Other concentration of Co^{2+} reacted with P*p*PD microparticles were also investigated (Fig.S3-S7†), the light scattering signal and structure features underwent a similar change with different rates, suggesting that in the corrosion

reaction, Co^{2+} concentration played a vital role. More interestingly, the slope (the scattering lights intensity of P*p*PD relative to Co^{2+} concentration) shows good linearity with the scattering lights intensity of P*p*PD. Fig.4 shows the slope of different Co^{2+} content reacted with P*p*PD microparticles, the slope value of each concentration is listed in Table S1. Coefficient of correlation also can be obtained from the table. The result suggested that the sensing sensitivity increased as the Co^{2+} concentration gets higher. At the same time, this result enables us to estimate the sensitivity of P*p*PD microparticles through their shape changes and scattering lights.

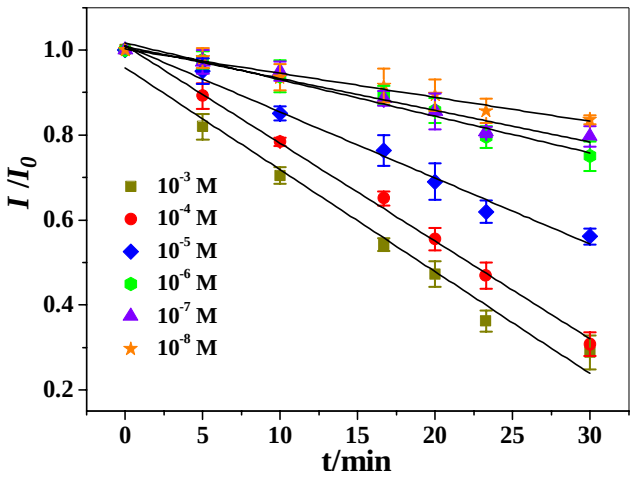

Fig. 4 Study of the effect on the light scattering intensity of single P*p*PD microparticle before and after exposure to different Co^{2+} concentrations. Error bars are calculated from measurements of three microparticles. I_0, the initial scattering light intensity of single P*p*PD microparticle. I the light scattering intensity of the same P*p*PD microparticle after reaction with Co^{2+} for different concentration.

The interaction between P*p*PD microparticles and Co^{2+} is identified to be a corrosion process. As SEM images shown in Fig. 5A, small eroded cracks appeared on the smooth surface of P*p*PD microparticles after the addition of Co^{2+}, which became much more evident with increasing Co^{2+} concentration. The shape of P*p*PD microparticles changed from leaf-like to irregular when Co^{2+} was 8.33×10^{-6} M (Fig. 5A (d)). When increased the concentration of Co^{2+}, these microparticles were completely eroded, leaving a few irregular fragments (Fig. 5A (f)).

In order to further obtain information about the dynamic of the corrosion process, we have performed concentration-resolved dynamic light scattering (DLS). The results coincide well with those obtained from the SEM and DFM images. It could be detectable that the average diameter of P*p*PD gradually decreased with the increasing content of Co^{2+} within the range from 0.33×10^{-6} to 11.7×10^{-6} mol/L. The linear regression equation is d =2596–186 c (where d is the size of P*p*PD, nm and c is the concentration of Co^{2+}, μmol/L) with the corresponding correlation coefficient (r) of 0.9941.

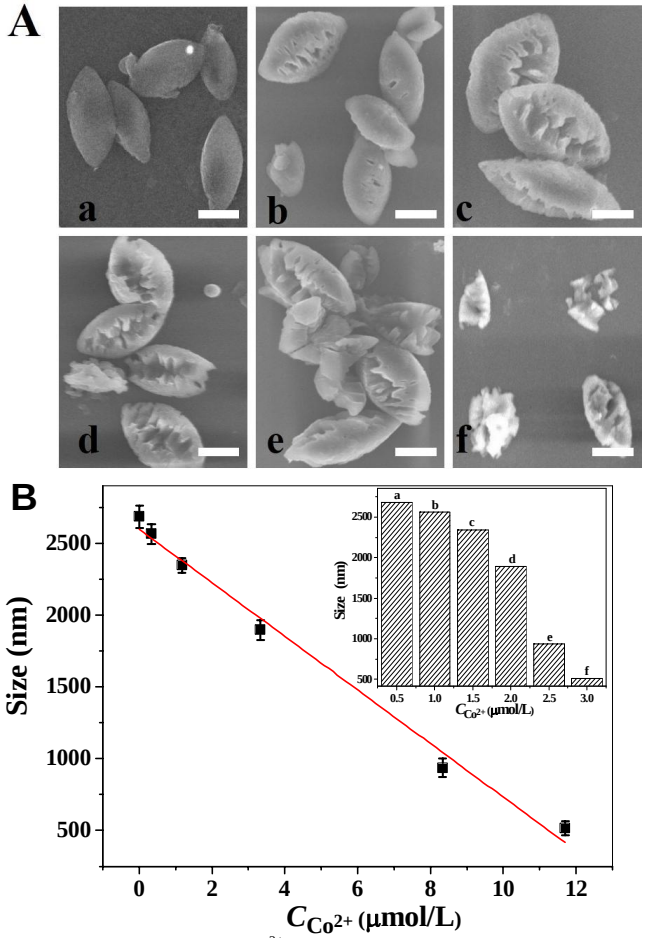

Fig. 5 (A) Eroding effect of Co^{2+} on the P*p*PD microparticles as displayed by SEM images; (B) Linear response of the size of the P*p*PD microparticles with the addition of Co^{2+}. $C_{Co^{2+}}$ (a-f, μmol/L) 0, 0.333, 1.17, 3.33, 8.33, 11.7. The SEM scale bar corresponds to 1 μm.

Conclusions

In summary, real-time monitoring of the corrosion of P*p*PD microparticles driven by Co^{2+} using dark-field scattering microscopy was reported. In this work, the P*p*PD acted as the sensing probe that reacted with Co^{2+}. Furthermore, P*p*PD microparticles functioned as the signal reporter, whose structure was broken and the scattering light was debilitated. The present study demonstrated the corrosion degree of the P*p*PD was correlated with the surrounding Co^{2+} concentration. As a result, the Co^{2+} concentration and their variations were able to be determined in real-time over a dynamic range of six orders of magnitude. The present work enables us to design a corrosion reaction based on probes with given optical property, and they are expected to be monitored at the single-particle level, thus making this method a valuable technique for the real-time monitoring of chemical reactions in analytical chemistry. Moreover, DFM was proven to be a powerful tool for real-time monitoring the process reaction.

To develop an exact theory of corrosion and accomplish the dynamic monitor is a challenging prospect. Some aspects for such a theory are discussed above and further investigation is in progress.

Acknowledgements

This work was financially supported by the Natural Science Foundation of China (21035005) and the Cultivation Plan of Chongqing Science & Technology Commission for 100 Outstanding Science and Technology Leading Talents.

Notes and references

[a] *Key Laboratory of Luminescence and Real-Time Analytical Chemistry (Southwes University), Ministry of Education, College of Chemistry and Chemical Engineering, Southwest University, Chongqing 400715, China. E-mail: chengzhi@swu.edu.cn, Tel: (+86) 23 68254659, Fax: (+86) 23 68367257.*

[b] *College of Pharmaceutical Science, Southwest University, Chongqing 400716, China*

† Electronic Supplementary Information (ESI) available: Experimental section and additional figures (Fig. S1-S6), table （Table S1）and moive S1. See DOI: 10.1039/b000000x/

1 G.A. Knauer, J.H. Martin and R.M. Gordon, *Nature*, 1982, **297**, 49-51.
2 M. Kobayashi and S. Shimizu, *Eur. J. Biochem.*, 1999, **261**, 1-9.
3 S. A. El-Safty, *Adsorption*, 2009, **15**, 227-239.
4 M. Gharehbaghi, F. Shemirani and M. D. Farahani, *J. Hazard. Mater.* 2009, **165**, 1049-1055.
5 A. R. Khorrami, T. Hashempur, A. Mahmoudi and A. R. Karimi, *Microchem. J.*, 2006, **84**, 75-79.
6 S. J. Zhen, F. L. Guo, L. Q. Chen, Y. F. Li, Q. Zhang and C. Z. Huang, *Chem. Comm.*, 2011, **47**, 2562-2564.
7 A. Afkhami, M. Abbasi-Tarighata and H. Khanmohammadi, *Talanta*, 2009, **77**, 995-1001.
8 J. L. Chen, A. F. Zheng, Y. C. Gao, C. Y. He, G. H. Wu, Y. C. Chen, X. C. Kai and C. Q. Zhu, *Spectrochim. Acta, Part A*, 2008, **69**, 1044-1052.
9 W. Y. Lin, L. Yuan, Z. M. Cao, J. B. Feng and Y. M. Feng, *Dyes Pigm.*, 2009, **83**, 14-20
10 S.H. Mashraqui, M. Chandiramani, R. Betkar and K. Poonia, *Tetrahedron Lett.*, 2010, **51**, 1306-1308.
11 D. Badocco, P. Pastore, G. Favaro and C. Macca, *Talanta*, 2007, **72**, 249-255.
12 S. L. Zhao, Y. Huang, M. Shi, J. Huang and Y.M. Liu, *Anal. Biochem.*, 2009, **393**, 105-110.
13 A. K. Singh, S. Mehtab and P. Saxena, *Sens. Actuators, B*, 2007, **120**, 455-461.
14 D.F. Marino, F. Wolff and J.D. Ingle Jr., *Anal. Chem.*, 1979, **51**, 2051-2053.
15 L. Zhang, J. M. Zhou, Y. H. Hao, P. G. He and Y. Z. Fang, *Electrochim. Acta*, 2005, **50**, 3414-3419.
16 Y. M. Leng, F. Q. Zhang, Y. J. Zhang, X.Q. Fu, Y.B. Weng, L.Chen and A. G. Wu, *Talanta*, 2012, **94**, 271-277.
17 F. Q. Zhang, L. Y. Zeng, Y. X. Zhang, H. Y. Wang and A. G. Wu, *Nanoscale*, 2011**, 3**, 2150-2154.
18 A.R. Khorrami, A.R. Fakhari, M. Shamsipur and H. Naeimi, *Int. J. Environ. Anal. Chem.*, 2009, **89**, 319-329.
19 W. Y. Lin, L. Yuan, L. L. Long, C. C. Guo and J. B. Feng, *Adv. Funct.Mater.* 2008, **18**, 2366-2372.
20 F. M. Rivera and J. Dumonceau, *Anal. Bioanal. Chem.*, 2002, **374**, 1105-1112.
21 Y. Liu and C. Z. Huang, *Nanoscale*, 2013, 5, 7458-7466.
22 J.Yguerabide and E. E. Yguerabide, *Anal. Biochem.*, 1998, **262**, 157-176.
23 C. Jing, Z. Gu, Y.-L. Ying, D.-W. Li, L. Zhang and Y.-T. Long, *Anal. Chem.*, 2012, **84**, 4284-4291.
24 W.-G. Qu, B. Deng, S.-L. Zhong, H.-Y. Shi, S.-S. Wang and A.-W. Xu, *Chem. Coumum.*, 2011, **47**, 1237-1239.
25 Y. Liu and C. Z.Huang, *Analyst*, 2012, **137**, 3434-3436.
26 L. Shi, C. Jing, W. Ma, D. –W. Li, J. E. Halls, F. Marken, Y. –T. Long, *Angew. Chem., Int. Ed.*, 2013, **125**, 6127-6130.
27 Y. Liu and C. Z.Huang, *Nanoscale*, 2013, **5**, 7458-7466.
28 L. Zhang, Y. Li, D.-W. Li, C. Jing, X.-Y. Chen, M. Lv, Q. Huang, Y.-T. Long and I. Willner, *Angew. Chem., Int. Ed.*, 2011, **123**, 6921 – 6924
29 Y. Liu and C. Z. Huang, *Chem. Coumum.*, 2013, **49**, 8262-8264.
30 S. Berciaud, L. Coget, P. Tamarat and B. Lounis, *Nano Lett.*, 2005, **5**, 515-518.
31 C. Novo, A. M. Funston and P. Mulavaney, *Nat. Nanotechnol.*, 2008, **3**, 598-602.
32 Y. Liu and C. Z.Huang, *ACS nano*, 2013, **7**, 11026-11034.
33 B. Xiong, R. Zhou, J.-R. Hao, Y.-H. Jia, Y. He and E. S. Yeung, *Nat. Commum.*, 2013, doi:10.1038/ncomms2722.
34 J. J. Wang, J. Jiang, B. Hu and S. H. Yu, *Adv. Funct. Mater.*, 2008, **18**, 1105-1111.
35 M. Brust, M. Walker, D. Bethell, D. J. Schiffrin and R. Whyman, *J. Chem. Soc., Chem. Commum.*, 1994, **7**, 801-802.
36 M. R. Dasog and W.J. Scott, *Langmuir*, 2007, **23**, 3381-3387.
37 H. Zitter, *J. Biomed. Mater. Res.*, 1987, **21**, 881-896.
38 D. Maity, R. Gupta, R. Gunupuru, D. N. Srivastava, P. Paul, *Sensors Actuat. B*, 2014, **191**, 757-764.
39 C. J. Murphy, T. K. Sau, A. M. Gole, C. J. Orendorff, J. Gao, L. Gou, S. E. Hunyadi and T. Li, *J. Phys. Chem. B*, 2005, **109**, 13857-13870.

Graphic abstract

for

A dark field light scattering platform with microparticles for real-time dynamic detection of Co^{2+}

Hui Yang,[a] Yue Liu,[a] Peng Fei Gao,[a] Jian Wang*[b] and Cheng Zhi Huang*[a,b]

[a] *Key Laboratory of Luminescence and Real-Time Analytical Chemistry (Southwest University), Ministry of Education, College of Chemistry and Chemical Engineering, Southwest University, Chongqing 400715, China. E-mail: chengzhi@swu.edu.cn, Tel: (+86) 23 68254659, Fax: (+86) 23 68367257.*

[b] *College of Pharmaceutical Science, Southwest University, Chongqing 400716, China*

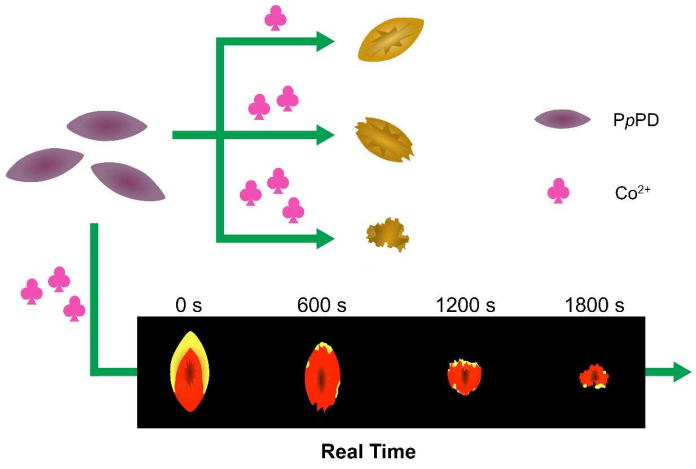

Poly (*p*-phenylenediamine) (P*p*PD) microparticles were prepared by the reported methods with slight modification, and then used for the quantitative detection of Co^{2+} with a dark-field microscopy technique based on the shape changes and light scattering signals of P*p*PD.